Journal of Thermal Science Vol.31, No.1 (2022) 111−119

https://doi.org/10.1007/s11630-022-1514-9 **Article ID: 1003-2169(2022)01-0111-09**

Research on Calculation Method of Aerodynamic Parameters of Supersonic Probe Based on Gas Compressibility Factor

ZHONG Jingjun, HUANG Gangfeng, WU Wanyang, KAN Xiaoxu*

Merchant Marine College, Shanghai Maritime University, 1550 Haigang Avenue, Pudong District, Shanghai 201306

Abstract: The supersonic multi-hole probe is an essential test tool for wind tunnel experiments, which is necessary to develop the basic research of improving the measurement accuracy and expanding the application of the probes.

This paper theoretically derived a gas compression factor $\delta_s \sim f(p^*, p_s, \kappa, \lambda)$ to expand the scope of application of Bernoulli's equation, and discussed the reliability issues of using this factor to solve the velocity and Mach number of the supersonic flow. The research results show that the calculation method of aerodynamic parameters of the supersonic flow proposed in this paper has credibility within one ten-thousandth of the calculation error compared with the calculation of aerodynamic theory. Compared with the algorithm in this paper and the other three algorithms, the calculation errors of the velocity and Mach number of the supersonic flow and the static pressure ratio before and after the shock are all within the range of one ten-thousandth based on the experimental data of a transonic turbine linear cascade. However, the error of the post-wave Mach number is relatively large. Finally, a universal supersonic multi-hole probe calibration algorithm proposed in this paper is suitable for automated non-opposing measurement. It has generally credible and fully considers the shock wave factor. It will improve the theoretical system of multi-hole probes, and provide theoretical guidance and technical support for the supersonic wind tunnel experiment.

Keywords: supersonic flow, probe, gas compressible factor, aerodynamic parameter, error analyses

1. Introduction

With the advancement of science and technology, flow field measurement technology has expanded from a single, traditional and contact probe measurement to an emerging, non-contact and optical measurement device, such as Particle Image Velocimetry measurement [1]. Compared with a probe that required a servo motor for stepping single-point measurement, optical measurement could achieve a full-area measurement only in one-time, and has the advantages of high spatial resolution, fast dynamic response, and good direction sensitivity. However, optical measurement needed to pass through the plexiglass window when entering the flow field of the engine without contact. Due to the limitation of the actual engine structure size, there would be the influence of the measurement viewing angle, ambient light, calibration, etc. Therefore, it was difficult to implement the complex flow field in the engine [2].

Compared with optical measurement that could only obtain a single velocity field or pressure field, the traditional probe could directly achieve measurement of the pressure, temperature and velocity of the flow, and has accurate measurement, simple measurement principle,

Article type: Contributed by Asian Congress on Gas Turbines 2020 (August 18–19, 2021, China).
Received: Oct 15, 2021 Corresponding author: KAN Xiaoxu E-mail: xxkan@shmtu.edu.cn

Nomenclature

Notation			
a	sound velocity	λ	velocity factor
h	gas enthalpy	$\pi(\lambda)$	aerodynamic function of pressure
K	calibration coefficient	ρ	flow density
Ma	Mach number	$\tau(\lambda)$	aerodynamic function of temperature
P	pressure	**Subscript**	
q	heat transfer per unit mass of fluid	s	static value
T	flow temperature	α	angle of pitch
v	flow velocity	β	deflection angle
γ	specific heat ratio	1	before the shock wave
δ_s	gas compression factor	2	behind the shock wave
$\varepsilon(\lambda)$	aerodynamic function of density	**Superscript**	
κ	adiabatic index	*	total value

and the equipment was relatively optical; furthermore, the instrument was simpler and more reliable [3]. Based on this, probe measurement was the measure standard for the correctness of optical measurement, and the basis for quantitative measurement. The probe was still the most used and convenient measurement method [4–6]. However, the current measurement principle of the probe was derived based on the Bernoulli equation of incompressible fluid. It can be known from the gas dynamics theory that when the Mach number of gas flow is greater than 0.3, the compressibility of the gas cannot be ignored; especially the degree of influence of the compressibility of the gas is particularly important, when flowing across supersonic velocity. The reliability and accuracy of the probe measuring the flow field puts forward new requirements.

Our previous research [7] theoretically solved the relative change rate of flow density $\mathrm{d}\rho/\rho=\left(\rho^*/\rho\right)-1=(1/2)Ma^2+\left[(2-\kappa)/8\right]Ma^4+\cdots$ (ρ is flow density; Ma is Mach number; κ is the specific heat ratio) and the relative change rate of temperature $\mathrm{d}T/T=\left(T^*/T\right)-1=\left[(\kappa-1)/2\right]Ma^2$ (where T and T^* are static temperature and total temperature) changing with the Mach number of the flow. It could be clearly recognized that the compressibility of gas and the increase in entropy due to shock waves couldn't be ignored from the high-subsonic to supersonic flow conditions. The measured values obtained by the probe measurement method based on the Bernoulli equation of incompressible fluid were quite different from the theoretically true values, and especially the errors at supersonic flow were beyond the acceptable range.

Is the correction method feasible that the application range of the current probe calibration data expanded by introducing the gas compression factor $\delta_s \sim f(p^*, p_s, \kappa, \lambda)$ for the transonic and supersonic flow conditions with shock wave phenomenon? It can be done by sorting out the derivation process of Bernoulli equation based on steady-state adiabatic isentropic flow theory. The theory is based on the universal enthalpy energy equation $q-\omega_s=(h_2-h_1)+(1/2)\left(v_2^2-v_1^2\right)$ (where q is heat transfer per unit mass of fluid; ω_s is axial work done per unit mass of fluid; h is gas enthalpy; v is gas velocity.) Some preconditions were introduced during the period:

$$\frac{1}{2}\left(V_2^2-V_1^2\right)\overset{\text{①}}{=}h_1-h_2\overset{\text{②}}{=}C_p\left(T^*-T\right)\overset{\text{③}}{=}\frac{\kappa}{\kappa-1}R\left(T^*-T\right)\overset{\text{④}}{=}\frac{\kappa R T^*}{\kappa-1}\left[1-\left(\frac{p^*}{p_s}\right)^{\frac{\kappa-1}{\kappa}}\right]$$

Ideal gas isentropic process relation pv^{κ}=const

Mayer's formula $C_p=\dfrac{\gamma}{\gamma-1}R_g=\dfrac{\kappa}{\kappa-1}R_g$

In the isentropic process, adiabatic index κ=specific heat ratio γ

As complete gas in the reversible process, $h=C_pT$

Not involve the specific situation of the gas in the control volume, and be applicable to whether the flow is reversible or not

For the transition from transonic to supersonic flow, there was a shock wave around the probe's head [8, 9]. The increase in entropy caused by the shock wave was an irreversible, adiabatic, unequal entropy process. Then, the calculation method based on the Bernoulli equation of steady adiabatic isentropic as the theoretical basis would not hold. In addition, the total pressure measured by the probe was the value behind the shock wave, which was less than the total pressure of the true incoming flow in the front of the shock wave, which would cause the total pressure coefficient to be a large negative value [10], and furthermore it leaded to the singularity encountered in the non-dimensionalities of calibration coefficients [11].

In summary, we need to establish a set of calibration formulas for probes that are suitable for transonic and supersonic flows, which is different from the current calibration formulas.

From the Rayleigh-pitot tube formula [12] $\frac{p_2^*}{p_{s1}}=\left(\frac{\gamma+1}{2}\right)^{\frac{\gamma+1}{\gamma-1}}\left(\frac{2}{\gamma-1}\right)^{\frac{1}{\gamma-1}}\frac{Ma_1^{\frac{2\gamma}{\gamma-1}}}{\left(\frac{2\gamma}{\gamma-1}Ma_1^2-1\right)^{\frac{1}{\gamma-1}}}$, the relationship among the total pressure (p_2^*), static pressure (p_{s1}) and Mach number (Ma_1) obtained by the probe in the conditions of transonic and supersonic flow was too complicated. The expression of the compression factor ε' in the calculation process of solving the flow velocity was as followed, which was not conducive to automated data processing:

$$\varepsilon'=\left(\frac{\gamma+1}{2}\right)^{\frac{\gamma+1}{\gamma-1}}\left(\frac{2}{\gamma-1}\right)^{\frac{1}{\gamma-1}}\frac{2Ma_1^{\frac{2}{\gamma-1}}}{\gamma\left(\frac{2\gamma}{\gamma-1}Ma_1^2-1\right)}-\frac{2+\gamma Ma_1^2}{\gamma Ma_1^2}$$

In this paper, we attempted to combine the compressibility $\varepsilon(p^*, p_s)$and temperature characteristic $f(T)$ of the gas produced by the shock wave into a dimensionless correction relation $f(p^*, p_s, T, \gamma)$. It was defined as a shock factor δ_s to simplify the supersonic probe calibration formula, so that its expression was closer to the current probe calibration formula in form. This will be a gas compression factor $\delta_s \sim f(p^*, p_s, \kappa, \lambda)$ that only needs to be calculated from the pressures reading from the probe holes to correct the current calculation method of the probe to solve the flow velocity. Thus, it can extend the applicable range of probe calibration data from low-speed flow to supersonic flow conditions. This can ensure the measurement accuracy, reduce the amount of calibration calculations, increase the test speed, shorten the experiment cycle, and provide theoretical support for the establishment of automatic non-opposing measurement of the supersonic multi-hole probe.

2. Calculation Method of Aerodynamic Parameters of Supersonic Probe

2.1 Limitations of the current solution of aerodynamic parameters before and after shock

In general, supersonic flow around the probe will inevitably generate a shock wave at the probe head. The probe can measure aerodynamic parameters such as total pressure P_2^* , static pressure P_{s2} and total temperature T_2^* after shock wave. In fact, what we need to obtain is the various aerodynamic parameters of the supersonic flow in front of the shock wave. Among them, because the shock wave is an adiabatic process, the total energy of the air flow before and after the shock wave is unchanged, that is, the total temperature before the wave T_1^* equals to the total temperature after the wave T_2^* . For this reason, it is also necessary to calculate the total pressure p_1^* and static pressure P_{s1} of the wave front through the measurable total and static pressure of the back wave.

First, the ratio of parameters before and after the normal shock wave in the gas dynamics theory is expressed as a function of the wave front Mach number.

$$\frac{p_{s2}}{p_{s1}}=\frac{2\gamma}{\gamma+1}Ma_1^2-\frac{\gamma-1}{\gamma+1}$$
$$\frac{p_1^*}{p_2^*}=\left(\frac{2\gamma}{\gamma+1}Ma_1^2-\frac{\gamma-1}{\gamma+1}\right)^{\frac{1}{\gamma-1}}\cdot\left(\frac{2}{\gamma+1}\frac{1}{Ma_1^2}+\frac{\gamma-1}{\gamma+1}\right)^{\frac{\gamma}{\gamma-1}} \tag{1}$$

where p_{s1} is the static pressure before the shock wave; p_{s2} is the static pressure behind the shock wave; p_1^* is the total pressure before the shock wave; p_2^* is the total pressure behind the shock wave

2.2 Derivation of gas compressibility factor

It can be seen from the above formula that if you want to obtain the total pressure p_1^* and static pressure p_{s1} before the shock wave, you need to know the wave front Mach number Ma_1 first. However, this cannot be achieved directly for multi-hole probe measurement.

Here, the aerodynamic function $\pi(\lambda_2)$ can be obtained by the total pressure p_2^* and static pressure p_{s2} after the wave, and then the velocity factor λ_2 after the wave can be obtained by inverse calculation. Then, it can be known from the Prandtl relation of positive shock waves, $\lambda_1\lambda_2=1$; therefore, the velocity factor of the wave front can be obtained. Next, we can use the velocity factor λ_1 in Eq. (1) to replace the Mach number Ma_1, and introducing the aerodynamic function $\tau(\lambda_1)$, and $\varepsilon(\lambda_1)$, we can get

$$p_1^*=p_2^*\cdot\lambda_2^2\frac{\varepsilon(\lambda_2)}{\varepsilon(\lambda_1)}\qquad p_{s1}=p_{s2}\cdot\lambda_2^2\frac{\tau(\lambda_1)}{\tau(\lambda_2)} \tag{2}$$

Secondly, in order to be able to unify the expression of the gas compression factor, it is assumed that the supersonic gas flow before the shock wave also conforms to the Bernoulli equation of the compressible fluid, that is, it satisfies

$$p_1^* = p_{s1} + \frac{1}{2}\rho_{s1} v_1^2 (1+\varepsilon) \tag{3}$$

At the same time, according to the definition of sound velocity a and the ideal gas state equation, we can get

$$v_1^2 = a_1^2 \cdot Ma_1^2 = \gamma \frac{p_{s1}}{\rho_{s1}} Ma_1^2 \tag{4}$$

Combining Eq. (3) and Eq. (4), we can get the expression about the gas compressibility:

$$1+\varepsilon = \frac{2\left(\dfrac{p_1^*}{P_{s1}} - 1\right)}{rMa_1^2} \tag{5}$$

where r is the specific heat ratio of the specific pressure heat capacity to the specific heat capacity.

For Eq. (5), the velocity factor λ_1 is used to replace the Mach number Ma_1, and the aerodynamic function is introduced to obtain a dimensionless gas compressibility correction factor (referred to as gas compressibility factor) suitable for supersonic flow, which is recorded as δ_s:

$$\delta_s = 1+\varepsilon = \frac{\gamma+1}{\gamma} \cdot \frac{\left[1-\pi(\lambda_1)\right]}{\lambda_1^2 \varepsilon(\lambda_1)} \tag{6}$$

The gas compression factor δ_s suitable for supersonic flow and the gas compression factor δ_ε [13] suitable for high subsonic flows are completely consistent in form, but the assumptions and basic equations of gas dynamics involved in the derivation process are different.

2.3 Calculation process of aerodynamic parameters of supersonic flow

The Bernoulli equation of supersonic flow can be expressed as:

$$p_1^* = p_{s1} + \frac{1}{2}\rho_{s1} v_1^2 \delta_s \tag{7}$$

In the formula, considering that it is more difficult to directly solve the density of the supersonic flow ρ_{s1} before the shock wave using only the limited aerodynamic parameters collected by the pneumatic probe; the aerodynamic function $\varepsilon(\lambda_1)$ is used as the transition variable to solve the problem, as follows:

$$\rho_{s1} = \varepsilon(\lambda_1)\rho_1^* = \varepsilon(\lambda_1)\frac{p_1^*}{RT_1^*} \tag{8}$$

In addition, the Mach number Ma_1 of the supersonic flow in front of the shock wave can be obtained by the velocity factor λ_1 and the aerodynamic function $\tau(\lambda_1)$:

$$Ma_1 = \sqrt{\frac{\dfrac{2}{\gamma+1}\lambda_1^2}{\tau(\lambda_1)}} \tag{9}$$

In summary, the calculation flow chart of using multi-hole probe to obtain supersonic velocity and aerodynamic parameters is shown in Fig. 1, where K_α and K_β are pitch angle coefficient and deflection angle coefficient respectively.

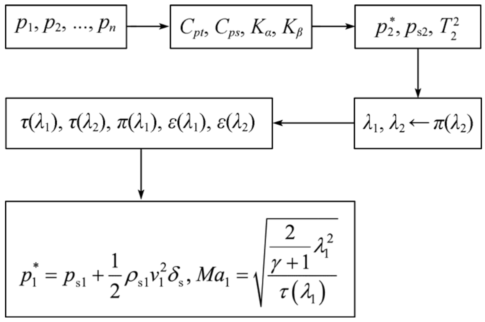

Fig. 1 Calculation process of aerodynamic parameters of supersonic flow

3. Verification of the Reliability of the Calculation Method

3.1 Verification with theoretical values of gas dynamics

In order to verify the credibility of the calculation formulae for the supersonic flow proposed above, the comparative analysis of the total pressure ratio and static pressure ratio between front and behind of shock wave are calculated from the normal shock properties as the standard values and these formulae, as shown in Fig. 2. Furthermore, the Mach number range of the incoming flow is selected from 1.0 to 1.6, and the calculation interval of Mach number is 0.5. The data of the total and static pressure ratios selected from the normal shock properties are represented by blue squares and red dots, while the ones obtained by the calculation formulae are represented by blue and red curves, respectively.

As the incoming Mach number increases, the total pressure ratio gradually decreases, while the static pressure ratio increases almost linearly. Furthermore, the change trends of both total pressure ratio and static pressure ratio obtained by these two methods are the same, and the values are almost equal. Further, the detailed calculation error analysis is shown in Fig. 3. Among them, the calculation error of the total pressure ratio is indicated by the blue histogram, and one of the static pressure ratios is indicated by the orange histogram. It shows that the total pressure ratio obtained by the calculation formula proposed in this paper has an error band of 0.0017% to 0.0024% compared with the value in the normal shock properties as the standard values. At the same time, the error band of the static pressure ratio is of –0.0035% to 0.0036%. These are very small quantifications and are within the allowable range of errors. Therefore, it can be proved that the calculation formulas of the total pressure ratio and static pressure ratio between front and behind the shock wave proposed in this paper are credible and are consistent with existing gas dynamics theories.

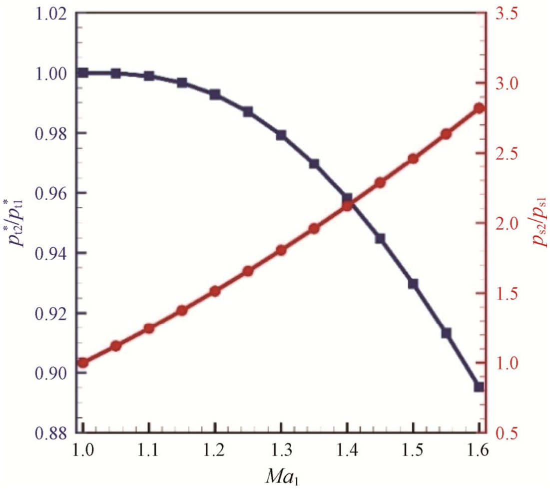

Fig. 2 Total and static pressure ratios between front and behind of shock wave with two methods

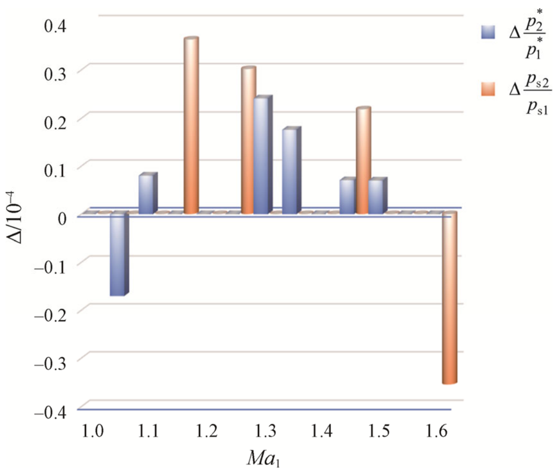

Fig. 3 Calculation error of the values in Fig. 2

3.2 Verification with experimental values of turbine cascade

The outlet aerodynamic parameters of the transonic turbine linear cascade in Ref. [14] to verify the credibility of the method to solve the flow velocity by the gas compressibility factor proposed in this paper. The blade profile selected in the experiment was composed of the cross-sectional blade profile of a highly-pressure turbine rotor blade. The cascade model was shown in Fig. 4, and the geometric parameters and aerodynamic parameters were shown in Table 1. The complete set of experimental blade cascades includes nine experimental blades made of steel, of which the passage composed of 4 and 5 blades was the experimental measurement passage to ensure the periodicity of the measurement. The inlet measuring section of the cascade was 1 time the chord length from the leading edge of the blade; the outlet measuring section was about 0.7 times the axial chord length from the trailing edge of the blade.

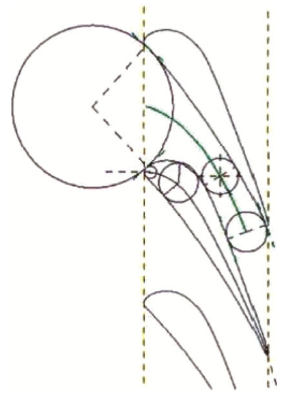

Fig. 4 Schematic diagram of the cascade [14]

Table 1 Geometrical parameters of the cascade

Parameter	Value
Solidity	1.72
Aspect ratio	1.67
Axial chord	33.05 mm
Throat width	9.65 mm
Stagger angle	33.6°
Inlet geometric angle	0°
Outlet geometric angle	73.5°

The experimental section of the cascade is shown in Fig. 5. The aerodynamic parameters such as air total pressure, static pressure, velocity, and Mach number on the outlet section of the cascade are obtained by a three-hole wedge-shaped pneumatic probe through a non-opposing measurement method.

In order to ensure the typicality of the verification of the air velocity solution method, this paper selects a working condition point belonging to transonic flow, where the angle of attack i=0° and the outlet isentropic Mach number Ma_{is2}=1.09 are set. The variations of the energy loss coefficient ξ and outlet deflection angle $\Delta\beta_2$ along the pitch direction of cascade outlet section at each working point are considered comprehensively. Finally, the measuring point position of the probe when the two aerodynamic parameters are the average value of the pressure surface (point A), the average value of the suction surface (point C and D), the maximum value (point B), the minimum value (point F) and in the mainstream area (Point E) is selected as the working condition point of this paper. The measuring point position of working condition point I is shown in Fig. 6.

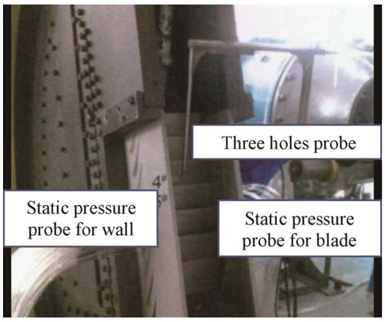

Fig. 5 Installation drawing of the cascade

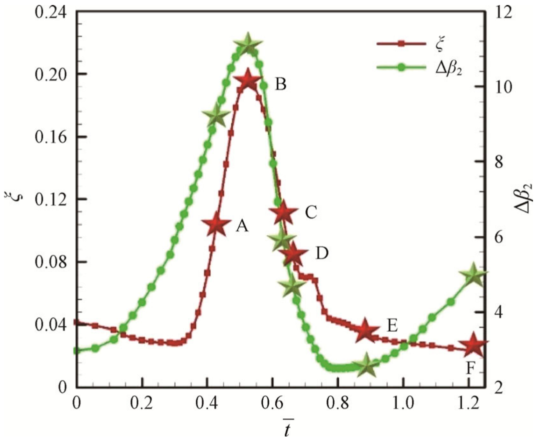

Fig. 6 Basis for selecting points for verification calculation

The Rayleigh-Pitot tube formula method (indicated by Ray in the following figures) is to bring the total static pressure ratio of the total pressure behind the shock and the static pressure before the shock into the Rayleigh-Pitot tube formula to obtain the Mach number Ma_1 before the shock. The positive shock table interpolation method (the figure below is represented by Pro) is to bring the total static pressure ratio between the total pressure behind the shock and the static pressure before the shock into the normal shock table. Then using this ratio of total static pressures as the initial value, the corresponding Mach number Ma_1 before the shock wave is calculated using the second-order Newton interpolation method. The calculation method used in Ref. [2] is also the calculation method commonly used in the current cascade wind tunnel experiment; that is, according to the aerodynamic function relationship of Mach number, the ratio of the total static pressure obtained by the direct measurement of the experiment is used to obtain the air flow Mach number. It should be noted that this method does not consider the existence of shock waves. In the end, the air velocity solving methods in the above three methods are all calculated by using the definition formula of Mach number. The flow of the three calculation methods is shown in Fig. 7.

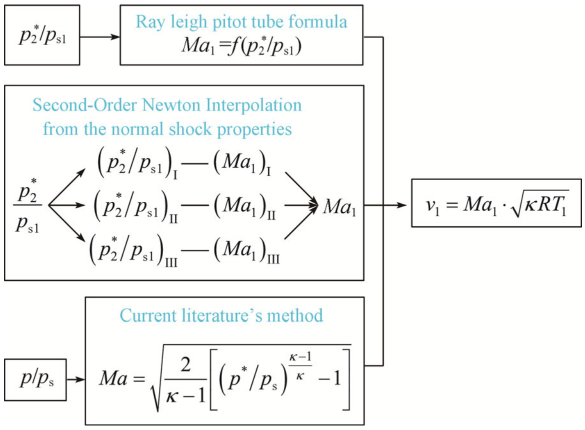

Fig. 7 Calculation process of other three methods

Furthermore, the second-order Newton interpolation method used in this paper specifically refers to, in the interval [1.8929, 3.8049]. The definition of the zero-order difference quotient of the first node $\left(p_2^*/p_{s1}\right)_{\mathrm{I}}$ of Mach number $Ma_1 \sim f\left(p_2^*/p_{s1}\right)$ before the shock wave with respect to the total static pressure ratio before and after the shock wave is shown in Eq. (10). $Ma_1 \sim f\left(p_2^*/p_{s1}\right)$ regarding the definition of the first-order difference quotient of two adjacent nodes $\left(p_2^*/p_{s1}\right)_{\mathrm{I}}$ and $\left(p_2^*/p_{s1}\right)_{\mathrm{II}}$ is shown in Eq. (11). In this paper, the second-order difference quotient is the difference quotient of the first-order difference quotient, and $Ma_1 \sim f\left(p_2^*/p_{s1}\right)$ about the second-order difference quotient of $\left(p_2^*/p_{s1}\right)_{\mathrm{I}}$, $\left(p_2^*/p_{s1}\right)_{\mathrm{II}}$, $\left(p_2^*/p_{s1}\right)_{\mathrm{III}}$ is Eq. (12). Specifically, the difference quotient can be calculated regularly according to the format of Table 2.

$$\left[Ma_1\right]_{\mathrm{I}} = \left(Ma_1\right)_{\mathrm{I}} \tag{10}$$

$$\left\{\left[Ma_1\right]_{\mathrm{I}}, \left[Ma_1\right]_{\mathrm{II}}\right\} = \frac{\left(Ma_1\right)_{\mathrm{II}} - \left(Ma_1\right)_{\mathrm{I}}}{\left(\frac{p_2^*}{p_{s1}}\right)_{\mathrm{II}} - \left(\frac{p_2^*}{p_{s1}}\right)_{\mathrm{I}}} \tag{11}$$

$$\left\{\left[Ma_1\right]_{\mathrm{I}}, \left[Ma_1\right]_{\mathrm{II}}, \left[Ma_1\right]_{\mathrm{III}}\right\} = \frac{\left\{\left[Ma_1\right]_{\mathrm{II}}, \left[Ma_1\right]_{\mathrm{III}}\right\} - \left\{\left[Ma_1\right]_{\mathrm{I}}, \left[Ma_1\right]_{\mathrm{II}}\right\}}{\left(\frac{p_2^*}{p_{s1}}\right)_{\mathrm{III}} - \left(\frac{p_2^*}{p_{s1}}\right)_{\mathrm{I}}} \tag{12}$$

With the help of the definition of the difference quotient, the second-order Newton interpolation polynomial when Mach number Ma1 before the shock wave can be expressed as:

$$N_n(x)=[Ma_1]_{\mathrm{I}}\,\omega_1(x)+\left\{[Ma_1]_{\mathrm{I}},[Ma_1]_{\mathrm{II}}\right\}\omega_2(x)+\left\{[Ma_1]_{\mathrm{I}},[Ma_1]_{\mathrm{II}},[Ma_1]_{\mathrm{III}}\right\}\omega_3(x) \tag{13}$$

where n is interpolating polynomial of order n, and x is the variable.

Among them,

$$\omega_1(x)=1,$$

$$\omega_2(x)=\left[x-\left(\frac{p_2^*}{p_{s1}}\right)_{\mathrm{I}}\right]\left[x-\left(\frac{p_2^*}{p_{s1}}\right)_{\mathrm{II}}\right],$$

$$\omega_3(x)=\left[x-\left(\frac{p_2^*}{p_{s1}}\right)_{\mathrm{I}}\right]\left[x-\left(\frac{p_2^*}{p_{s1}}\right)_{\mathrm{II}}\right]\left[x-\left(\frac{p_2^*}{p_{s1}}\right)_{\mathrm{III}}\right]$$

Table 2 Calculation process of difference quotient

$(p_2^*/p_{s1})_k$	$(Ma_1)_k$	first-order	second-order
$(p_2^*/p_{s1})_{\mathrm{I}}$	$(Ma_1)_{\mathrm{I}}$	–	–
$(p_2^*/p_{s1})_{\mathrm{II}}$	$(Ma_1)_{\mathrm{II}}$	$\{[Ma_1]_{\mathrm{I}}, [Ma_1]_{\mathrm{II}}\}$	–
$(p_2^*/p_{s1})_{\mathrm{III}}$	$(Ma_1)_{\mathrm{III}}$	$\{[Ma_1]_{\mathrm{II}}, [Ma_1]_{\mathrm{III}}\}$	$\{[Ma_1]_{\mathrm{I}}, [Ma_1]_{\mathrm{II}}, [Ma_1]_{\mathrm{III}}\}$

There are four methods that using the Rayleigh-Pitot tube formula method, the normal shock properties interpolation method (Pro), the current commonly used algorithm and the Bernoulli equation algorithm. It introduces a compression factor of supersonic flow proposed in this paper to solve the flow velocity and Mach number of transonic flow (operating condition point I), shown in Fig. 8. In the measuring points in this paper, except that the local flow Mach number at point B is less than 1.0, which is a high subsonic flow, the air flow Mach numbers of the other measuring points are all greater than 1.0, which are typical transonic flows. This is because the measurement point B is in the core of the cascade wake region, where a large number of low-energy fluid clusters accumulate, so the flow velocity is the lowest. The flow Mach number and velocity at each measuring point calculated by the above four algorithms are not much different in value, and the law of change trend is completely consistent.

Fig. 9 and Fig. 10 show the relative error values of the flow Mach number and velocity obtained by the algorithm proposed in this paper and the other three algorithms mentioned above, respectively. Furthermore, the ordinate is processed, and one ten-thousandth of the original data is displayed on the coordinate axis.

The ratio of the Mach number Ma_1 between the compression factor algorithm and the current common algorithm is between -5.5×10^{-15} and 7.6×10^{-15}. It can be seen that the error is very small, which is an acceptable error range and has good compatibility. Although the error of these two algorithms is slightly larger, the error is between 0.003% and 0.004%, which is an acceptable error range due to the impact of shock wave. The error of Mach number ΔMa_1 and ΔV_1 between the compression factor algorithm and the Rayleigh-Pitot tube formula method is between –0.002 79% and –0.002 71%, which is an acceptable error range, indicating that the compression factor is consistent with the theoretical formula considering the impact of shock waves.

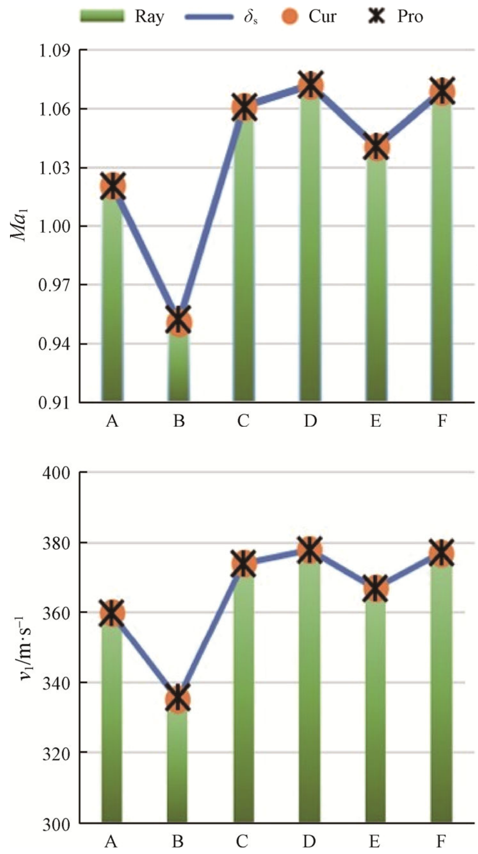

Fig. 8 Comparison of the Mach number and velocity in condition I obtained by using different four algorithms

The error of Mach number ΔMa_1 between the compression factor and the normal shock properties interpolation method (Pro) is mostly between –0.004 63% and 0.000 32%, which is an acceptable error range. However, the error value of these two algorithms at point B is –0.184%. This error value is obviously larger than that of other points. The reason is that point B is in the wake of the cascade, which is the accumulation of a large number of low-energy fluid clusters. In the region, the Mach number of the local flow Ma_B=0.953, which belongs to the state of high subsonic flow. Based on this, it can be considered that the calculation method proposed in this paper will have large errors in the calculation of high subsonic flow. At the same time, the error of ΔV_1 obtained by the two algorithms is slightly larger than the Mach number ΔMa_1, between –0.015 56% and 0.012 27%, which may be caused by the error of the interpolation remainder, but it is still the acceptance range. This shows that the second-order Newton interpolation is credible and the calculation is simple.

In summary, it can be considered that the compression factor algorithm proposed in this paper considers the shock wave and has a small error with the current algorithm. It is a credible method to find the flow's velocity and Mach number.

3.3 Verification of the reliability of aerodynamic parameters after shock

The static pressure ratio $\Delta \dfrac{p_{s2}}{p_{s1}}$ and the shock wave Ma_2 are obtained through the compression factor algorithm and the normal shock properties interpolation method (Pro). The purpose is to further verify the reliability of the compression factor algorithm, and the error between the two methods is shown in Fig. 11. It can be seen from the figure that the error of static pressure ratio $\Delta \dfrac{p_{s2}}{p_{s1}}$ is mostly about –0.001 54% to –0.000 59%, and the error is very small which is acceptable. The error of ΔMa_2 after shock wave is –0.000 84% to 0.003 21%, which is slightly larger but acceptable. ΔMa_2 is slightly larger due to the shock wave generated at the probe head at supersonic flow. The shock wave form is not explained publicly in the literature, especially in the transonic process where it has multiple shock waves. So the next step is to focus on the shock wave spectrum of the probe head.

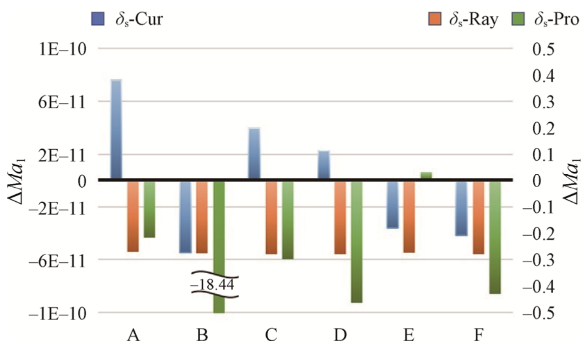

Fig. 9 Relative error of the incoming Mach number in Fig. 8

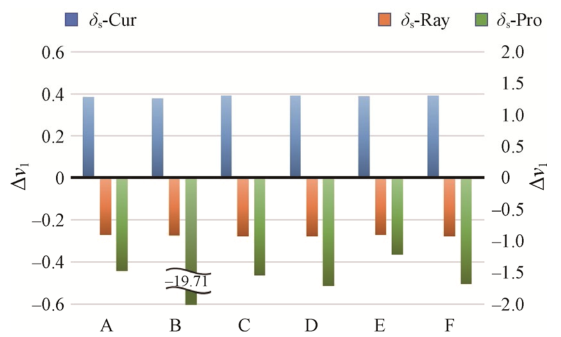

Fig. 10 Relative error of the incoming velocity in Fig. 8

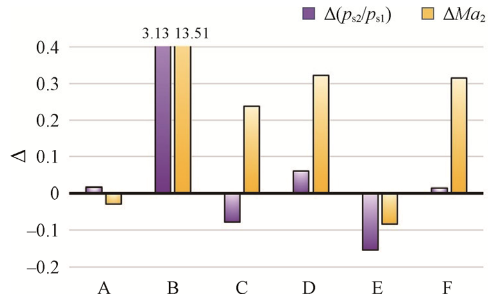

Fig. 11 Relative error of static pressure ratio and Mach number back the shock wave obtained by two algorithms

4. Conclusions

(1) This paper used the values of the total/static pressures on the probe head after the shock wave, and established the function between the aerodynamic parameters before the shock wave and the velocity factors after the shock wave with the Prandtl relationship formula. Then, the expression of the gas compressibility factor suitable for supersonic flow was derived by transforming the Bernoulli equation of the aerodynamic parameters before the shock wave. Finally, a more convenient and universal method for calculating supersonic aerodynamic parameters was obtained.

(2) Compared with the data in the normal shock properties, the calculation error of the total/static pressure ratios before and after the shock wave obtained by the calculation method proposed in this paper were both within the range of one ten thousandth, indicating that the algorithm was reliable and consistent with the gas dynamics theory.

(3) Compared with the current literature's method, the Rayleigh-Pitot tube formula method, and the normal shock properties interpolation method, the algorithm proposed in this paper was used to calculate the supersonic flow velocity and Mach number from the test data of the transonic turbine linear cascade The calculation errors were all within one ten-thousandth, but the calculation errors when solving the velocity and Mach number of high subsonic flow were relatively larger, which is not within the acceptable range. This showed that this algorithm for solving supersonic flow was credible, and the shock wave factor was fully considered.

(4) The errors of static pressure ratio before and after

shock and Mach number after shock obtained by the algorithm proposed in this paper and the normal shock properties interpolation method were both within one ten thousandth, which is acceptable range. However, the error of the Mach number after shock was relatively larger, which might because the structure of multiple shock in the transonic process has not been fully grasped. It is suggested that the future research topic should pay attention to the development of the shock wave structure of the supersonic probe head.

Acknowledgments

This study was co-supported by the National Natural Science Foundation of China (No. 51906134 and 51436002).

References

[1] Vergine F., Maddalena L., Stereoscopic particle image velocimetry measurements of super-sonic, turbulent, and interacting streamwise vortices: challenges and application. Progress in Aerospace Sciences, 2014, 66: 1–16.

[2] Johansen E.S., Rediniotis O.K., Jones G., The compressible calibration of miniature multi-hole probes. Journal of Fluids Engineering, 2001, 123(1): 128–138.

[3] Delhaye D., Paniagua G., Fernández Oro J.M., et al., Enhanced performance of fast-response 3-hole wedge probes for transonic flows in axial turbomachinery. Experiments in Fluids, 2011, 50(1): 163–177.

[4] Payne F.M., Ng T.T., Nelson R.C., Seven-hole probe measurement of leading-edge vortex flows. Experiments in Fluids, 1989, 7(1): 1–8.

[5] Sumner D., Heseltine J.L., Dansereau O.J.P., Wake structure of a finite circular cylinder of small aspect ratio. Experiments in Fluids, 2004, 37(5): 720–730.

[6] Gilarranz J.L., Ranz A.J., Kopko J.A., et al., On the use of five-hole probes in the testing of industrial centrifugal compressors. Journal of Turbomachinery, 2005, 127(1): 91–106.

[7] Kan X.X., Huang G.F., Wu W.Y., Zhong J.J., Research on solving flow velocity method of a high subsonic probe. Academic Conference on Thermomechanical and Aerodynamics of Chinese Society of Engineering Thermophysics; Baoding, Hebei, China, 2020, Oct 23–25, No. 202446. (in Chinese)

[8] Goodyer M.J., A stagnation pressure probe for supersonic and subsonic flows. Aeronautical Quarterly, 1974, 25(02): 91–100.

[9] Hsieh T., Flow-field study about a hemi-sphere-cylinder in the transonic and low supersonic Mach number range. AIAA Paper, 1975, 75–83: 1–11.

[10] Zhao B., Zhao J., Numerical simulation of pressure probe calibration based on CFD under supersonic condition. Metrology & Measurement Technology, 2017, 37(2): 15–18, 36. (in Chinese)

[11] Pisasale A.J., Ahmed N.A., Theoretical calibration for highly three-dimensional low-speed flows of a five-hole probe. Measurement Science & Technology, 2002, 13(7): 1100.

[12] Anderson J.D., Fundamentals of aerodynamics. Beijing: Aviation industry press, 2010, 3: 549–550.

[13] Zhong J.J., Kan X.X., Wu W.Y., et al., A composite pressure-temperature probe and flow velocity calculation method. China, 202010599342.5.

[14] Luo W.W., Wang H.S., Zhao X.L., Experiment investigation on the flow characteristic in a transonic convergent-divergent turbine cascade. Journal of Engineering Thermophysics, 2013, 34(7): 1229–1233. (in Chinese)